Title
OPEN FILE REPORT GEOSCIENCE STUDIES IN BUENA VISTA VALLEY, NEVADA

Authors
Goldstein, N. E.
Beyer, H.
Corwin, R.
et al.

Publication Date
1976-12-01

586
3-11-77
UC-66b

Di. 788

LBL-5913
UC-66b
TID-4500-R65

MASTER

Energy and Environment Division

Open File Report Geoscience Studies in Buena Vista Valley, Nevada

N. E. Goldstein, H. Beyer, R. Corwin, D. E. di Somma, E. Majer, T. V. McEvilly, H. F. Morrison, H. A. Wollenberg, and R. Grannell

December 1976

Lawrence Berkeley Laboratory University of California/Berkeley

Prepared for the U.S. Energy Research and Development Administration under Contract No. W-7405-ENG-48

LBL-5913

DISTRIBUTION OF THIS DOCUMENT IS UNLIMITED

Printed in the United States of America
Available from
National Technical Information Service
U.S. Department of Commerce
5285 Port Royal Road
Springfield, Virginia 22161
Price: Printed Copy $5.00; Microfiche $2.25

DISCLAIMER

LBL-5913

OPEN FILE REPORT

GEOSCIENCE STUDIES IN BUENA VISTA VALLEY, NEVADA

N. E. Goldstein, H. Beyer, R. Corwin, D. E. di Somma,
E. Majer, T. V. McEvilly, H. F. Morrison, and H. A. Wollenberg

University of California
Lawrence Berkeley Laboratory
Berkeley, California 94720

and

R. Grannell
California State University
Long Beach, California 90840

December 1976

This work was done with support from the U. S. Energy Research and Development Administration.

TABLE OF CONTENTS

OPEN FILE REPORT:
GEOSCIENCE STUDIES IN BUENA VISTA VALLEY, NEVADA

INTRODUCTION

As part of the study of applications of geoscience techniques to the assessment of potential geothermal resource areas, the Lawrence Berkeley Laboratory and the University of California, Berkeley have conducted geological, geophysical, and geochemical surveys in Buena Vista Valley, north-central Nevada. In this report we present results of these surveys and offer a preliminary interpretation of the data. The bases for the geophysical techniques employed were discussed in an earlier report on the Grass Valley area (Beyer, et al., 1976), and are not reported here. However, this information will be covered in detail in topical reports, scientific papers and research theses in preparation. Geochemical data acquired in our northern Nevada studies are being summarized and will be evaluated in a subsequent report (Bowman, et al., in preparation), but a brief summary of geochemical analyses of samples from the Buena Vista Valley area is presented here. Results of heat flow measurements in the Kyle Hot Springs area are described in some detail by Sass, et al. (1976); heat flow results are only briefly summarized in this report.

Kyle Hot Springs are located in Pershing County, 65 km south-southwest of Winnemucca, and 55 km east-northeast of Lovelock, the county seat. The area studied is on the eastern side of Buena Vista Valley within the Kyle Hot Springs Quadrangle, as shown in Figure 1.

GEOLOGIC SETTING

A geologic map of the Kyle Hot Springs Quadrangle (Figure 2) was compiled from observations by LBL personnel, reconnaissance mapping by Muller, et al. (1951), and air-photo interpretation by Noble (1974). Figure 3 is the accompanying idealized geologic cross-section (Z-Z'). Roberts, et al. (1958) provided lithologic descriptions of the rock units.

Pre-Tertiary basement rocks, exposed in the East Range to the east of the study area, consist of Paleozoic eugeosynclinal and Mesozoic miogeosynclinal rocks. The Harmony Formation, of Cambrian age, is the oldest exposed unit in the area and crops out in a small area on the north side of Hot Springs Canyon. It consists of feldspathic sandstone, arkose and grit with some chert. Most of the East Range in the Kyle Hot Springs Quadrangle is underlain by the Ordovician Valmy Formation. The Valmy consists of phyllitic argillite, greenstone and a pure vitreous quartzite, which caps some of the minor ridges in the northern part of the quadrangle. The Inskip Formation, primarily graywacke and conglomerate of Mississippian age, occurs in the upper part of Hot Springs Canyon. These Paleozoic eugeosynclinal rocks have been thrust over a crystalline limestone unit of probable Triassic age, exposed for about 5 km along the range front south of Hot Springs Canyon.

The East Range is capped by vesicular basalt of Tertiary age, which dips gently eastward and covers the east flank of the range in the adjacent Mt. Tobin Quadrangle. Granite Mountain, which projects westward into Buena Vista Valley in the southern part of the quadrangle, is composed of two masses of granitic rocks; the northern unit is a quartz monzonite of Tertiary age (Silberman and McKee, 1971), and the southern unit is a granodiorite of Permo-Triassic age.

Tertiary sedimentary rocks crop out in only one small area, of about 1 km^2, along the range front north of Granite Mountain. We assume that these sedimentary rocks and possible associated volcanic rocks underlie the Quaternary alluvium of the valley floor. The thickness of alluvium increases valleyward from the East Range, reaching 2 to 2-1/2 km in the central part of Buena Vista Valley (Erwin, 1974). Pleistocene shorelines of Lake Lahontan contour the valley a few kilometers west of Kyle Hot Springs. The active hot springs are presently depositing predominantly $CaCO_3$, although opalized sinter is abundant in older deposits and predominates at the inactive "fossil" hot springs area a few kilometers south of the active springs.

Both the active and inactive hot springs occur in an area of numerous intersecting faults. Air photo and on-site observations by Noble (1974) indicate that Kyle Hot Springs are localized by intense faulting and fault intersections; these are indicated on the geologic map, Figure 2. A prominent system of normal-fault scarps follows the western front of the East Range, northward from Granite Mountain, passing east of Kyle Hot Springs. Another prominent fault system trends southward from near the mouth of Klondike Canyon, thence southwestward to pass through the active hot springs. This system continues southwestward through the old, now inactive, spring area. The active and inactive spring areas at Kyle, then, are situated within a belt about 2 km long by 1 km wide which contains an unusually large number of faults and fault intersections. Another intense zone of intersecting faults is apparent in alluvium at the western end and northwestern edge of Granite Mountain. However, fracturing here does not appear as intense as at Kyle Hot Springs.

GEOCHEMISTRY

A compilation of geochemical data on rocks and waters of the Buena Vista Valley area is in progress (Bowman, et al., in preparation). Major element abundances in water from Kyle Hot Springs have been analyzed by Mariner, et al. (1974). Surface spring flow was measured at 20 l min^{-1}; spring water temperature reaches 77°C. Temperatures at depth within the spring system are estimated to be within the range 170 to 190°C, based on silica and alkali-element geothermometers.

A filtered water sample from Kyle Hot Springs was analyzed for some trace elements by the neutron activation method (Bowman, et al., 1975). Results are listed in Table I, together with trace element abundances in water from a cold spring in Hot Spring Canyon of the East Range.

Table I

	U (ppb)	W (ppb)	Mo (ppb)	Sb (ppb)	Ba (ppb)	Na (ppb)	Cl (ppb)
Kyle Hot Spring	*	80±15	*	8±1	550±50	569±13	721±17
Cold Spring	2.90±.04	*	2.5±.8	*	67±14	76±2	77±2
(* indicates below the dectectibility limit.)							

Comparison indicates that the hot spring water is nearly an order of magnitude higher than the cold spring in Ba, Na, and Cl, and the hot spring contains appreciable tungsten and antimony. Conversely, the cold spring water contains appreciable uranium and molybdenum.

As with other hot springs where $CaCO_3$ is the predominant deposit, Kyle Hot Springs are relatively high in radioactivity, compared with springs where SiO_2 is being deposited (Wollenberg, 1974). The Radon-222 content of a sample of the hot spring waters, collected in 1974 was 587 pCil^{-1}. Field measurements over the surface away from the hot pools at Kyle indicated

γ-ray exposure-rate background values of 12.5 to 25 μRhr^{-1}, while readings over the pools ranged from 250 to 500 μRhr^{-1}. Material presently being deposited on the walls of the hot spring is also relatively high in radioelement content, compared to older travertine away from the spring, as shown in Table II.

Table II
Radioelement Content of Spring Deposit Materials

	Th (ppm)	Equivalent U (ppb)	K (%)	Ra* ($pCig^{-1}$)
Calcareous Muck From Spring Walls	11.6	76.3	0.16	27
Travertine Away From Active Spring	0.2	4.1	0.09	1.5
(* Calcualted from activities ratio $^{226}Ra/^{238}U$.)				

GEOPHYSICS

Geophysical surveys conducted in Buena Vista Valley include gravity, magnetic, self-potential, electric-field-ratio telluric, dipole-dipole resistivity, and microearthquake surveys, as well as heat flow measurements. For all but the seismic and heat flow work, the geophysical data were collected along the eleven survey lines shown in Figure 4. With the exception of Line A-A', the lines trend normal to the strike of the range-front fault system, and several of the lines were extended into the East Range, following access routes provided by canyons.

In this section we discuss the results of the geophysical surveys, presenting the data in contour form where possible. Geophysical data profile composites for all lines are given in Appendix A.

Gravity Survey

Gravity data were obtained with a Lacoste-Romberg gravimeter at 204 stations, covering approximately 100 square-kilometers in Buena Vista Valley. Traverse lines were extended into the East Range within Klondike-Sulfur Canyons and French Boy Canyon. In general, a station interval of 500 meters was maintained along traverse lines.

Station elevations were estimated from topographic maps to an accuracy of ± 2 feet in the valley and ± 10 feet on the alluvial fans. Elevation accuracy of ± 5 feet was estimated at bedrock stations with known elevations.

The complete Bouguer anomaly, corrected for topography, was calculated using a Bouguer density of 2.67 g/cm^3. The contoured data are shown in Figure 5 (stations shown as dots) and profile data are shown in the composites of Appendix A. It is estimated that nearly all the values are accurate to better than ± 0.6 mGal.

The principal feature of the Bouguer anomaly map is the general decrease in gravity westward into Buena Vista Valley. This is interpreted as due to the progressive thickening of the Tertiary sediments filling the Basin and Range valley. The -35 mGal difference between the gravity minimum in Sec. 32, T.29N. R.36E. and the gravity values at outcropping Paleozoic sediments of the East Range suggests a valley fill thickness of 2.0 to 2.8 kilometers, assuming an average density contrast of 0.4 to 0.3 g/cm^3. This estimate agrees closely with that given by Erwin (1974) who interpreted a regional gravity survey. However, both estimates could be in error if the valley fill contains compacted and denser layers.

Two kilometers north of McClure Canyon, the gravity contours near the East Range abruptly change direction from northeast- to northwest-trending. This change closely matches a directional change of the East Range/alluvium contact.

The gravity contours near the present Kyle Hot Springs show a "nosing" effect of 2 mGal which may be due to a small, shallow zone of hydrothermally altered rock and spring deposits. A broader and more subtle bulge in the gravity contours occurs one to two km southwest of Kyle Hot Springs, in the vicinity of an inactive hot spring. This gravity effect, which appears as 5 mGal convexity in Profile C-C' (Fig. A3), may be due to a larger and deeper volume of silicified rock, and some modelling work is needed to obtain a better geological explanation for the anomaly. It is interesting that the anomaly occurs not only in an area of numerous intersecting faults, but is (a) coincident with a local increase in E-field-ratio (Figures A2 and A3) and (b) occurs on the edge of a 150 gamma magnetic high. The gravity, electrical and magnetic anomalies and the observed faulting are presumed to have a causal relationship to the near-surface heat source.

Near the center of the East Range, gravity values on lines D-D' and G-G' abruptly become more negative. This reversal is presumed to be due to a real, shallow structural feature.

Magnetic Survey

A Geometrics Model G816 proton precession magnetometer with a 1 gamma accuracy was used for a ground magnetic survey which covered an area of approximately 65 square-kilometers in the Buena Vista Valley and the adjacent western edge of the East Range. Readings were taken at 500-meter intervals along most lines in the valley, but the station separations were reduced to 200 or 125 meters where the lines crossed areas of steeper magnetic relief in the East Range. A contour map based on 65 line-kilometers of readings is shown in Figure 6, and profile data are shown in Appendix A. A contour interval of 100 gammas is used for the valley portion of the survey area, and a contour interval of 200 gammas is used in areas of steep magnetic relief. A base station correction was applied to all readings, and the relative accuracy of individual readings is assumed to be better than 10 gammas.

Kyle Hot Springs occurs in an elongate, northerly-trending magnetic low with gentle magnetic relief. Line B-B' passed directly over the hot spring, which Figure A2 shows is centered in the magnetic low. Three kilometers southwest of Kyle Hot Spring, in Sec. 10, T.29N., R.36E., a magnetic high of some 150 gammas was crossed by lines A-A' and B-B'. This feature also appears as a weak aeromagnetic anomaly in the U. S. Geological Survey Open File Aeromagnetic Map, Unionville Region, Pershing County, Nevada (1968). The magnetic high may be due to a horst of basement rock, interbedded Tertiary volcanics, or a concealed intrusive. According to a simple half-width estimate the source depth is one kilometer.

At the eastern margin of the survey area, over a region of Valmy Formation in the East Range, the magnetic field becomes extremely erratic, exhibiting numerous high-frequency changes of 100 to 1500 gammas (Figures A3, A4). These affects are "smoothed" in the contour map because of low station density, and thus are not accurately shown in Figure 6. To examine the field changes more closely, we ran a detailed magnetic profile along the eastern extension of Line B-B', and surveyed a small detailed grid (120 x 300 meters) near 2.375 E, Line C-C'. These surveys showed that the magnetic features have spatial wavelengths of 50 to 100 meters, and we suspect that the effects are due to mafic volcanics within greenstone units of the Valmy Formation (Silberling and Roberts, 1962).

Self Potential Survey

Five self-potential (SP) lines (A-A', B-B', D-D', F-F' and G-G') were run in the Buena Vista Valley, extending into the East Range. These data are shown on the profile composites of Appendix A (Figs. A1, A2, A4, A5, and A6). No anomalous SP activity was detected in the valley, but a very large negative anomaly was detected on all lines, beginning immediately west of the range front and extending into the East Range. The anomaly reaches -540 to -570 mV on the northernmost lines, decreasing to -320 mV on Line G-G'. The width of the anomaly ranges from about 5 to 7 km, and the width also appears to decrease southward. Preliminary results, not presented here, on lines run north of D-D' indicate that the anomaly continues to gain amplitude and width northward. The eastern half of line B-B' was surveyed separately by two field crews and, even though the measuring sites were not identical, Fig. A2 shows that the survey results were reproducible.

The width of the anomaly is at least an order of magnitude greater than typical SP anomalies caused by conductive mineralization, and its amplitude is toward the high end of the range for such anomalies. The only other reported SP anomaly of similar scale was measured in the Long Valley, California geothermal area (Anderson and Johnson, 1976), but the source of that anomaly is yet unknown.

Heat flow holes KY-1 and KY-3 (Fig. 9) were drilled in the area of the SP anomaly. The heat flow readings for the two holes are considered normal for the Battle Mountain regional heat flow anomaly (Sass et al., 1976). However, graphitic and pyritic Valmy Formation was intersected in KY-3, and a graphitic limestone was intersected in KY-1. This mineralogy could explain not only the SP anomaly, but also some of the coincident high conductivity anomalies; e.g., the dipole-dipole resistivity and E-field-ratio lows at roughly 2 km east, Line D-D' (Fig. A4), and the E-field-ratio low at Station 0, Line B-B' (Fig. A2).

It is reported (Hohmann, personal communication) that Bear Creek Mining Company (Kennecott) has also encountered graphitic, pyritic limestones in Nevada which cause resistivity lows and strong induced polarization effects.

These rocks could pose an interpretational problem for a geothermal exploration program should they occur in bedrock beneath a thin cover of valley fill. However, the SP technique provides a low-cost and rapid means for mapping the extent of these anomalies, thus providing some discrimination based on anomaly size and shape, between a possible geothermal system and a formational effect. Additional work is needed to determine the full extent of the SP anomaly, and the depth and dimensions of the source, but we are reasonably sure that the anomaly does not relate to thermoelectric or streaming potential effects from a geothermal source.

Electric-Field-Ratio Telluric Survey

The electric-field-ratio telluric method was used as an electrical reconnaissance technique in the vicinity of Kyle Hot Springs in Buena Vista Valley. In this method, natural telluric fields are measured by means of a tripole electrode array* that is advanced along a survey line. The electric fields between dipoles (dipole length of 500 m) are ratioed to yield the relative amplitude of the component of the E-field strength in the direction of the survey line. For this work the telluric signal was narrow bandpass filtered at two frequencies, 8 Hz and 0.05 Hz (20-second period), to provide some depth discrimination.

The telluric results are shown in the profile composites ofAppendix A (Figs. A1-A10). In the profiles the relative positions of the 8 Hz and 0.05 Hz traces are completely arbitrary with respect to the "relative electric field strength" axis. Additional discussion of the E-field-ratio telluric method was given by Beyer, et al. (1976).

---

*Two co-linear dipoles with one common electrode.

A total of 86 line-kilometers of telluric data were obtained at one-half-kilometer intervals along eight survey lines. Most of the lines are oriented perpendicular to the range-front fault system and the alluvium-bedrock contact, the direction for which orientation and polarization changes in the incident magneto-telluric source-field will not affect E-field-ratio telluric anomalies.

The telluric data on lines B-B', C-C', F-F', G-G', J-J', and L-L' (Figs. A2, A3, A5, A6, A7 and A8) show a common feature: decreasing E-field from east to west due to an increasing thickness of conductive sediments extending westward from the East Range. The longer period (0.05 Hz) telluric field should be affected more by basement rocks, while the 8 Hz field is normally affected by the overlying sediments. In the usual case of conductive sediments overlying a more resistive basement complex, the long period data should not fall off as quickly as the 8 Hz data, as was observed along Lines B-B', C-C' and J-J'. However, Lines G-G' and L-L' show the opposite trend, which suggests that the alluvium may contain lenses or layers more resistive than the underlying rocks.

The large negative SP anomalies, which are associated with graphitic and pyritic rocks along the western margin of the East Range, correspond to E-field-ratio anomalies. The 0.05 Hz telluric data generally show a low associated with this self-potential anomaly, as seen on Lines A-A' (dry electrodes), B-B', D-D' and F-F' and suggested on Line G-G'. The longer period tellurics appear to respond to this feature beginning 2.5 km south of the SP anomaly on Line A-A' and 2.5 km west of the SP anomaly on Line D-D'. Thus, the conductive body causing the self-potential anomaly in the East Range may continue westward under the Tertiary valley fill. The increasing thickness of alluvium should mask the self-potential anomaly at the surface, and therefore, the SP source may be broader than can be measured at the surface. Between 2.5 and 5 km west on Line D-D' both the telluric data and the dipole-dipole data (Fig. A4) indicate a near-surface resistivity high in the alluvium. This would further shield deep SP currents from the surface.

Kyle Hot Springs appears in the telluric data as a one point low at 3 km west on Line B-B' (Fig. A2). The electrode at this location was within 50 meters of the hot spring pools.

At 3 to 3.5 km west, Line L-L' crossed a relic sinter deposit located about 1.2 km southwest of Kyle Hot Springs and along the fault system which apparently controls the springs. At this location, the 0.05 Hz tellurics shows a relative high, suggesting either that resistive sinter extends to depth, or that there is particularly conductive material at depth east of the high, at 2.5 km west. The gravity data (Fig. 5) suggest a possible sinter mass. The low in the 8-Hz telluric profile at 3.5 km west indicates a low conductivity zone near the surface, associated with the sinter.

Dipole-Dipole Resistivity

A -500 mV self-potential anomaly and a coincident telluric low occur at the Star Point Mine on Line D-D', where alluvium is at most a thin veneer at the center of Klondike Canyon (Fig. A4). In an effort to discover the possible source of the large SP effect and to determine whether a conductive anomaly exists at depth at this location in the East Range, an in-line dipole-dipole survey was performed using one-km-length dipoles out to a maximum separation of ten dipole-lengths. The survey results are shown in Figure A4 in the standard form of an apparent-resistivity pseudo-section. (For a discussion of the dipole-dipole resistivity method and its interpretation see Beyer, et al. (1976)).

A preliminary attempt to find a two-dimensional fit to the pseudo-section was carried out by means of computer modeling. Figure 7 shows the resistivity model and the corresponding calculated pseudo-section obtained after several iterations. Although the modeling fit to the field data needs further refinement, the calculated pseudo-section depicts the general features seen in the field data; alternating high and low apparent-resistivity trends extending diagonally from upper right to lower left; the shallow resistive high at 3.5 km west; and the large apparent-resistivity low region extending down and to the west from the Star Point Mine (1 to 2 km east).

The resistivity model suggests that the pseudo-section data are controlled by very conductive (one ohm-meter) material at or near the bedrock surface. Three such bodies are shown in the resistivity model, two at the surface between 2 and 6 km east, and one at depth between 0 km and 4 km west. Geologic mapping and shallow drilling (heat flow hole KY-3 in the vicinity of Klondike Canyon) have revealed graphitic and pyritic rocks which may account for both the SP and conductivity anomalies.

A better fit between observed and calculated apparent resistivities might be obtained by moving the deepest conductive body eastward up the bedrock dip slope to the vicinity of 1 km west to 1 km east. This should have several desired effects: the low apparent resistivities at the eastern end of Line D-D' should move up to smaller N spacings; the 5 ohm-meter "alluvium" zone could be made thinner east of 1.5 km west, which would be consistent with the gravity data; the apparent resistivity values at depth beneath 3.5 km west should decrease to values more consistent with the field data.

An important point to note is that low apparent resistivities at large N spacings ("deep" in a pseudo-section) do not necessarily represent conductive bodies at depth. It appears that the low apparent resistivity anomaly below 3.5 km west at a dipole separation of N = 8 is caused by the existence of two near-surface conductive features: a graphitic, pyritic body in bedrock between 1 km west and 1 km east, and a thick section (∿ 1 km) of conductive sediments west of 6 km west.

Seismology

Seismological investigations were limited in Buena Vista Valley to two reconnaissance microearthquake surveys, each about two weeks in duration. Portable smoked-paper MEQ-800 seismographs were used in both surveys, in an initial attempt to locate possible source regions of microearthquake activity in the vicinity of Kyle Hot Springs. The stations were distributed as shown in Figure 8, in arrays extending to some 10 km from the hot springs area. In the first survey, conducted 2-12 September 1973, eight seismographs were deployed. A single earthquake was detected, located about 1.5 km south of the hot springs. The station network was operating at relatively high sensitivity, and would have detected any earthquakes of magnitude zero or greater within 10-15 km of the hot springs. A second reconnaissance survey, using five of the same seismographs, was conducted 26 August-8 September 1976 on the chance that the 1973 survey sampled a period of anomalously low seismicity. No earthquakes were detected in the second survey.

Had significant microearthquakes been detected in either survey, a 12-station network, with data telemetered and recorded on magnetic tape, would have been installed in the area. This system is required for meaningful subsequent studies of variations of attenuation, velocity, and ground noise throughout the area, and for precise hypocenter locations and source mechanism analyses.

It is conceivable that swarm-type microearthquake activity occurs, but it was not detected in the two 2-week surveys which may have unfortunately coincided with quiet periods. The single event lends credence to this possibility. Additional surveys were not conducted near Kyle Hot Springs because the field program was concentrated at the time in Grass Valley, where abundant seismic activity was occurring.

Heat Flow

As part of a joint LBL-USGS program, heat-flow measurements were planned near Kyle Hot Springs to see if the large SP anomalies (described earlier in this report) indicated the presence of a circulating hydrothermal system or were due to possible conductive mineralization in the bedrock on the western flank of the East Range. The heat-flow measurements and results are described in a recent open-file report (Sass et al., 1976), and are briefly summarized here.

Five heat-flow holes were initially planned: two were to be collared in phyllite and quartzite of the Valmy Formation, one in carbonate rock of probable Triassic age, and two in Quaternary alluvium west of Kyle Hot Springs. Only one hole (KY-3) was ultimately drilled in the Valmy Formation. The locations of the four holes drilled, together with heat flow values, are shown in Figure 9.

Inspection of cores and cuttings from hole KY-3, which penetrated $\sim$ 100 meters of Valmy Formation at Star Point Mine (Figure 1), indicated numerous graphite bands, as well as appreciable sulphide mineralization below a near-surface zone of oxidation $\sim$ 30-meters thick. Hole KY-1, drilled in the carbonate rock exposed on the south side of Hot Springs Canyon, encountered a $\sim$ 1-meter-thick zone of graphite, about 31 meters below the surface, and several thinner graphitic bands at other depths.

Table III lists estimated heat flows over depth intervals of constant geothermal gradient using thermal conductivities determined from cores and samples of drill cuttings. Heat flows in holes KY-1, KY-3, and KY-5 are similar to other heat flows measured in the "Battle Mountain High" (Sass et al., 1971). Because heat flow in the bedrock holes appears normal for the region, it is unlikely that the electrical geophysical anomaly on the western flank of the East Range indicates the presence of a hydrothermal system in that area.

Heat flow in hole KY-4 is greater than regional background, with an especially high value in the upper 65 meters of the hole. It is probable that this somewhat elevated heat flow results from the proximity of the hole to Kyle Hot Springs, only 2 km to the east. The hole is likely to be within the zone of circulating hydrothermal fluids associated with the hot springs.

Table III

Heat Flows Over Quasi-Linear Sections of Temperature Profiles, Kyle Hot Springs Area

Hole	Depth Interval (m)	Temperature Gradient °CKm^{-1}	N*	Thermal Conductivity (mcalcm^{-1}sec^{-1}°C^{-1})	Heat Flow (μcalcm^{-2}sec^{-1})
KY-1	37 - 96	38.70 ± 0.05	9	8.53 ± 0.25	3.30 ± 0.10
KY-3	18 - 100	34.77 ± 0.10	24	10.95 ± 0.44	3.81 ± 0.15
KY-4	23 - 67 75 - 137	136.7 ± 0.2 84.2 ± 0.1	16 27	4.98 ± 0.15 5.87 ± 0.19	6.8 ± 0.2 4.95 ± 0.16
KY-5	75 - 152	87.69 ± 0.05	29	3.63 ± 0.09	3.18 ± 0.08

*N is number of thermal conductivity determinations.

SUMMARY AND CONCLUSIONS

Within the survey area there is no visible indication of present-day hydrothermal activity except at Kyle Hot Springs. The geophysical work, consisting of gravity, magnetics, self-potential, E-field-ratio tellurics, dipole-dipole resistivity, microearthquake and heat flow measurements, did not detect evidence for any other circulating hot-water system.

Surveys conducted close to Kyle Hot Springs show that the spring activity corresponds to a single-point low in the E-field-ratio profiles and a weak gravity anomaly, due possibly to densification by precipitating spring deposits. No SP anomaly was found along a line over the hot springs.

An inactive "fossil" hot springs area lies one to two kilometers south of Kyle Hot Springs. Both inactive and active spring areas are characterized by intense faulting and numerous fault intersections. A broad 5 mGal gravity anomaly associated with the inactive springs may be due to denser hot spring deposits extending to depth. This occurrence is also suggested in the 0.05 Hz E-field-ratio data which show a corresponding resistivity high.

A third area of intersecting faults lies 13 km south of Kyle Hot Springs, in the alluvium at the western end of Granite Mountain. This area was not investigated because of constraints of time and our emphasis on higher priority areas.

One of the most intriguing geophysical features in the survey area was the large negative SP anomaly (-300 to -570 mV) paralleling the western margin of the East Range. Follow-up E-field-ratio telluric and dipole-dipole resistivity surveys showed that the SP source also has a low resistivity. Two heat flow holes, KY-1 and KY-3, were collared in the SP anomaly. Heat flow values were normal for the region, and drill cores and cuttings confirmed that SP and conductivity anomalies are most probably due to pyritic and/or graphitic zones in the rocks and not due to thermoelectric or streaming potentials related to hydrothermal activity.

A single microearthquake was detected $\sim$ 1.5 km south of Kyle Hot Springs during four weeks of monitoring. It is possible that swarm-type activity occurs and that our field work coincided with quiet periods.

Four heat flow holes were drilled but only one, KY-4, gave heat flow values greater than the regional background. This hole, two km southwest of Kyle Hot Springs, gave 6.8 HFU in the upper portion (23 to 67 m), declining to $\sim$ 5.0 HFU in the deeper portion (75 to 137 m). It has been suggested that the measured heat flow values are influenced by near-surface warm waters flowing down a hydrogeologic gradient from Kyle Hot Springs.

ACKNOWLEDGMENTS

The authors gratefully acknowledge the help of several people in conducting the field surveys. Ray Solbau, Milton Moebus, Donald Lippert, Warren Harnden, Robert Davis, and Bill Black of LBL provided the lion's share of technical support in the geoelectrical surveys. Paul Kolling and Stephen Palmer of the UCB Engineering Geoscience Group, and Joab Ndombi of Stanford University aided in the geoelectrical and magnetic surveys. The authors would also like to acknowledge Frank Olmsted, U. S. Geological Survey, Menlo Park for providing computer time for the reduction of the gravity data.

REFERENCES

Anderson, C. A. and Johnson, G. R., 1976, Application of the self-potential method to geothermal exploration in Long Valley, CA; Jour. Geophys. Res., V. 81, No. 8, p. 1527.

Beyer, H., et al., 1976, Preliminary open file report, geological and geophysical studies in Grass Valley, Nevada; Lawrence Berkeley Lab. Report LBL-5262.

Bowman, H., et al., 1975, Trace, minor, and major elements in geothermal waters and associated rock formations (north-central Nevada); in Proceedings of Second U. N. Symposium on the Development and Use of Geothermal Resources.

Erwin, J. W., 1974, Bouguer gravity map of Nevada: Winnemucca Sheet, Nevada Bur. Mines and Geol. Map 47.

Mariner, R. H., et al., 1974, The chemical composition and estimated minimum thermal reservoir temperatures of the principal hot springs of northern and central Nevada; U. S. Geol. Surv. open file report.

Muller, S. W., et al., 1951, Geology of the Mount Tobin Quadrangle, Nevada, U. S. Geol. Surv. Map GQ-7.

Noble, D. C., 1974, Reconnaissance study of the geological setting and fault control of the Kyle Hot Springs geothermal area; report to LBL Geothermal Group.

Roberts, R. J., et al., 1958, Paleozoic rocks of north-central Nevada, Bull. Amer. Assoc. Petroleum Geologists, V. 42, No. 12, p. 2813.

Sass, J. H., et al., 1971, Heat flow in the western United States: Jour. Geophys. Res., V. 76, No. 26, p. 6376.

Sass, J. H., et al., 1976, Heat flow near Kyle Hot Springs, Buena Vista Valley, Nevada; U. S. Geol. Surv. open file rept. 76-862.

Silberling, N. J. and Roberts, R.J., 1962, Pre-Tertiary stratigraphy and structure of northwestern Nevada, Geol. Soc. Amer. special paper 72.

Silberman, M. L., and McKee, E. H., 1971, K-Ar ages of granitic plutons in north-central Nevada, Isochron/West, No. 71-1, p. 15.

Wollenberg, H. A., 1974, Radioactivitiy of Nevada hot-spring systems, Geophys. Res. Lett., V. 1, No. 8, p. 359.

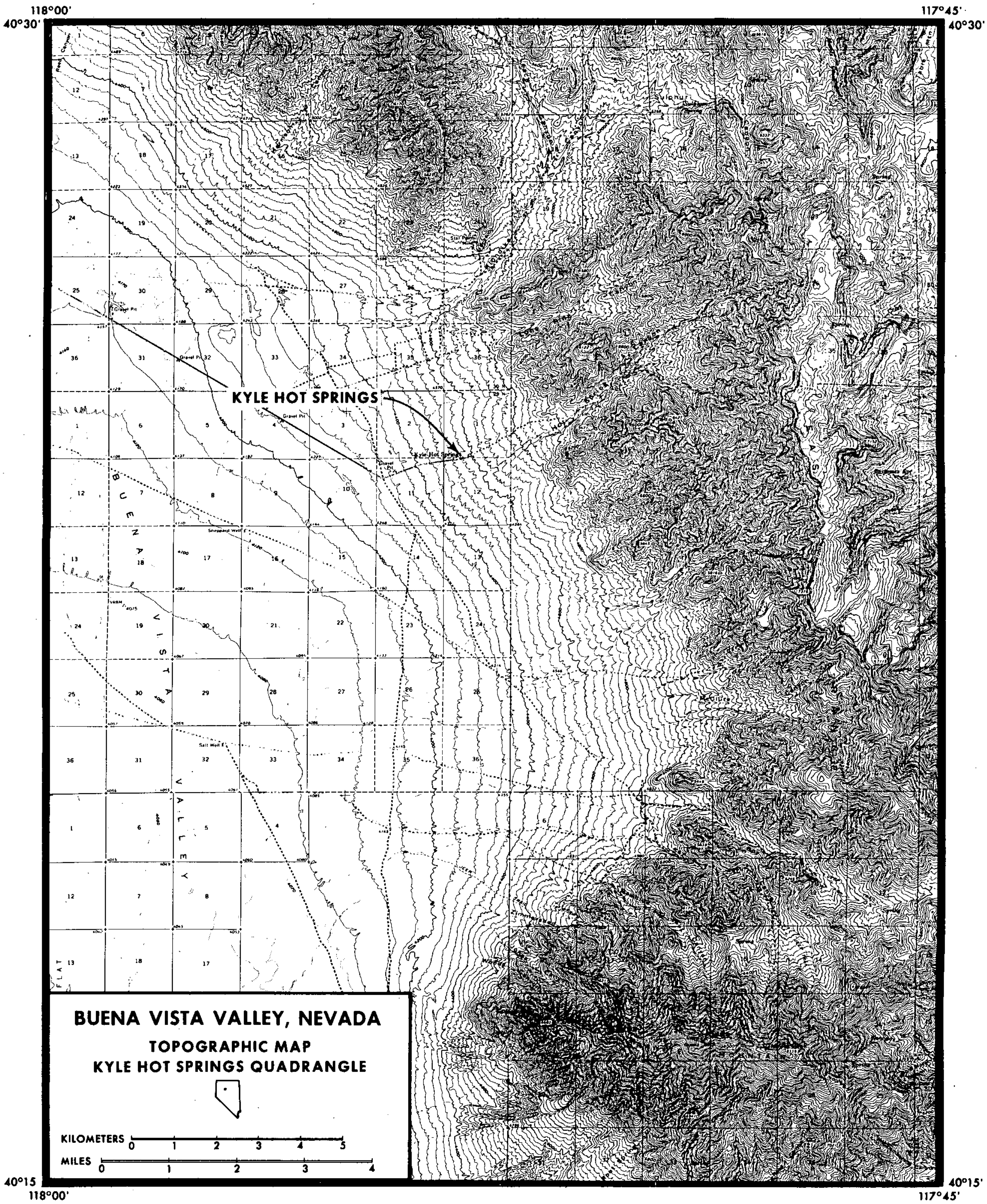

XBL 7612-10935

Figure 1

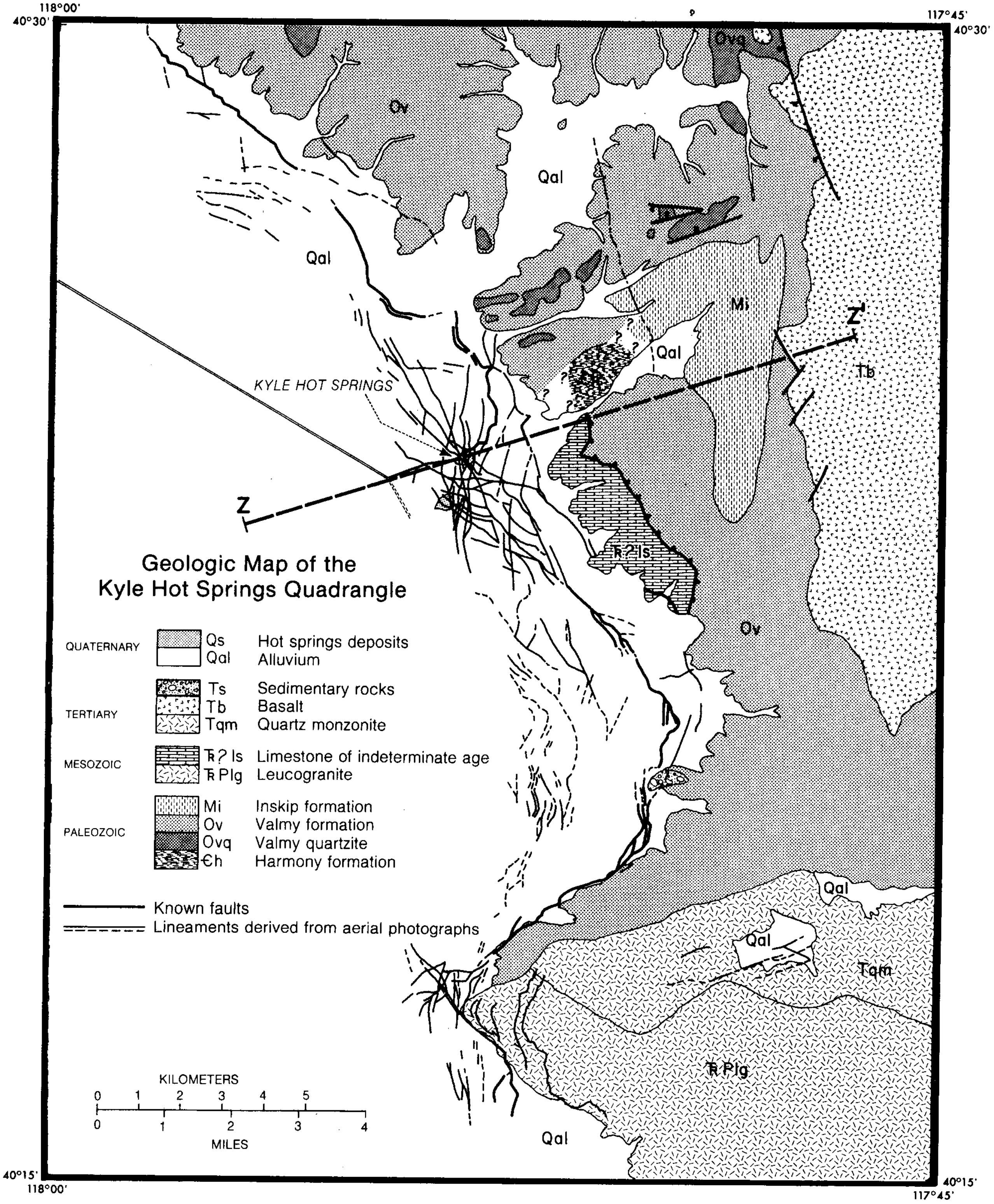

Figure 2

XBL 7611-4415

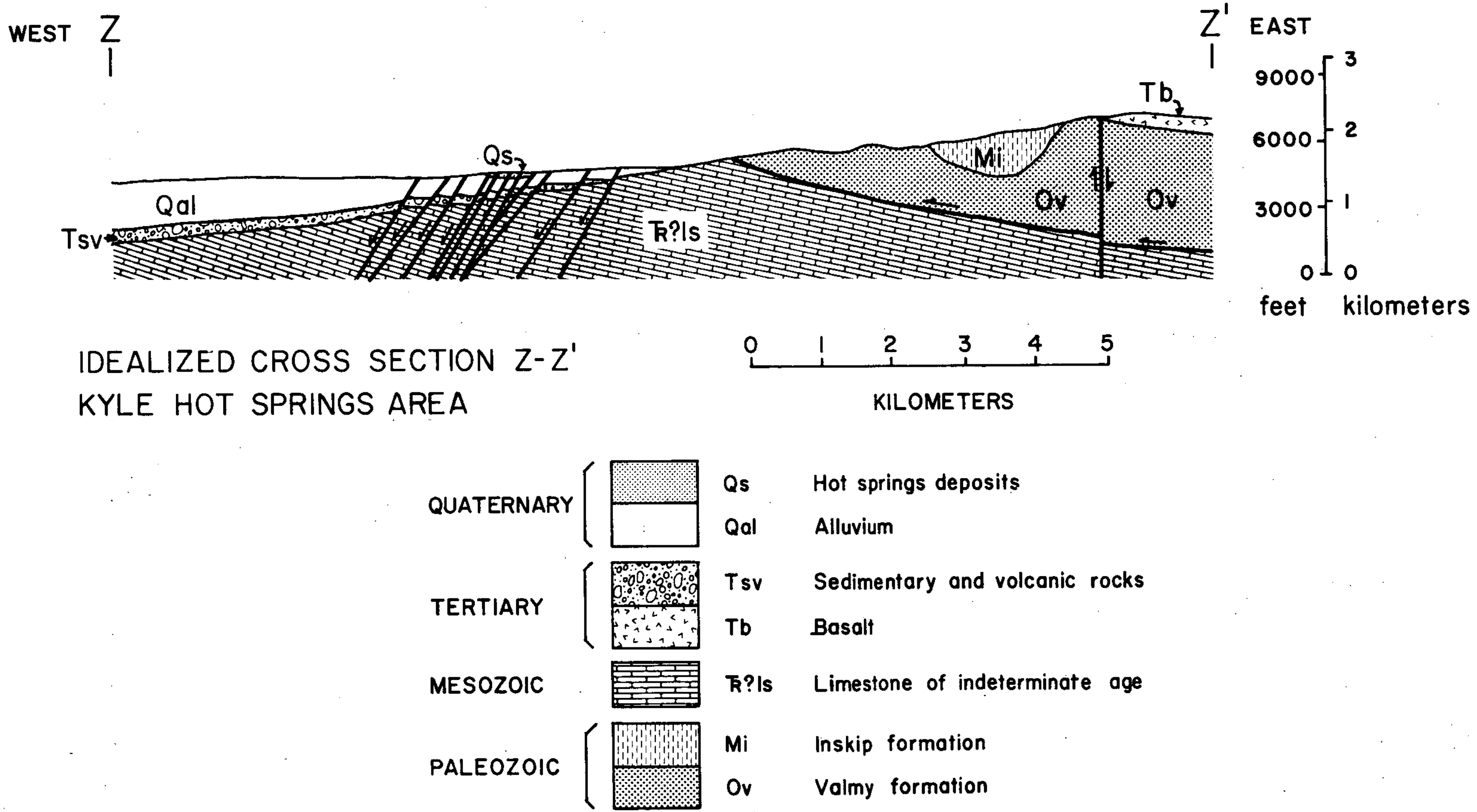

XBL 7612-10937

Figure 3. Idealized Geologic Cross Section, Buena Vista Valley and East Range, Pershing County, Nevada.

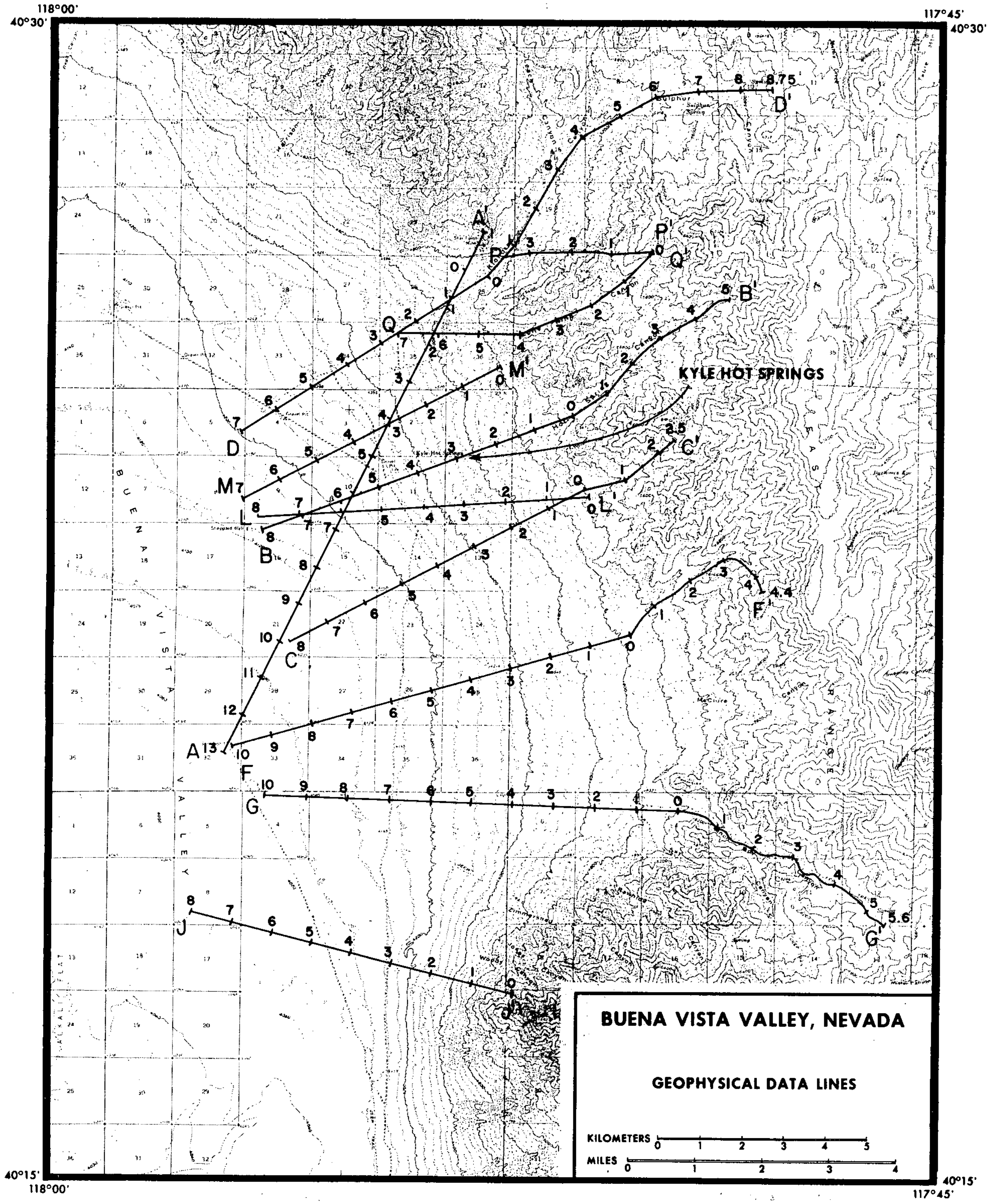

Figure 4

XBL 7612-10923

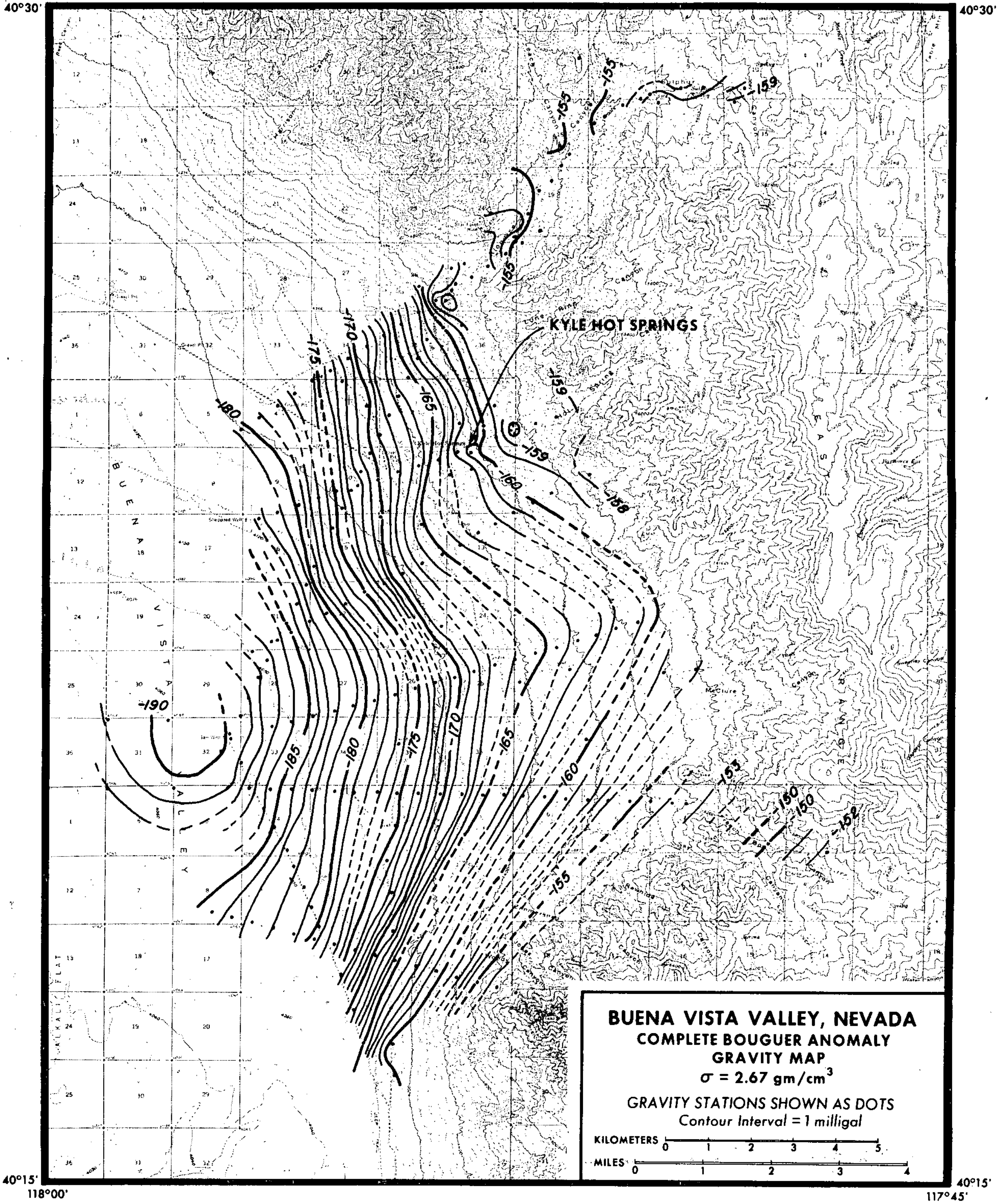

Figure 5

XBL 7612-10926

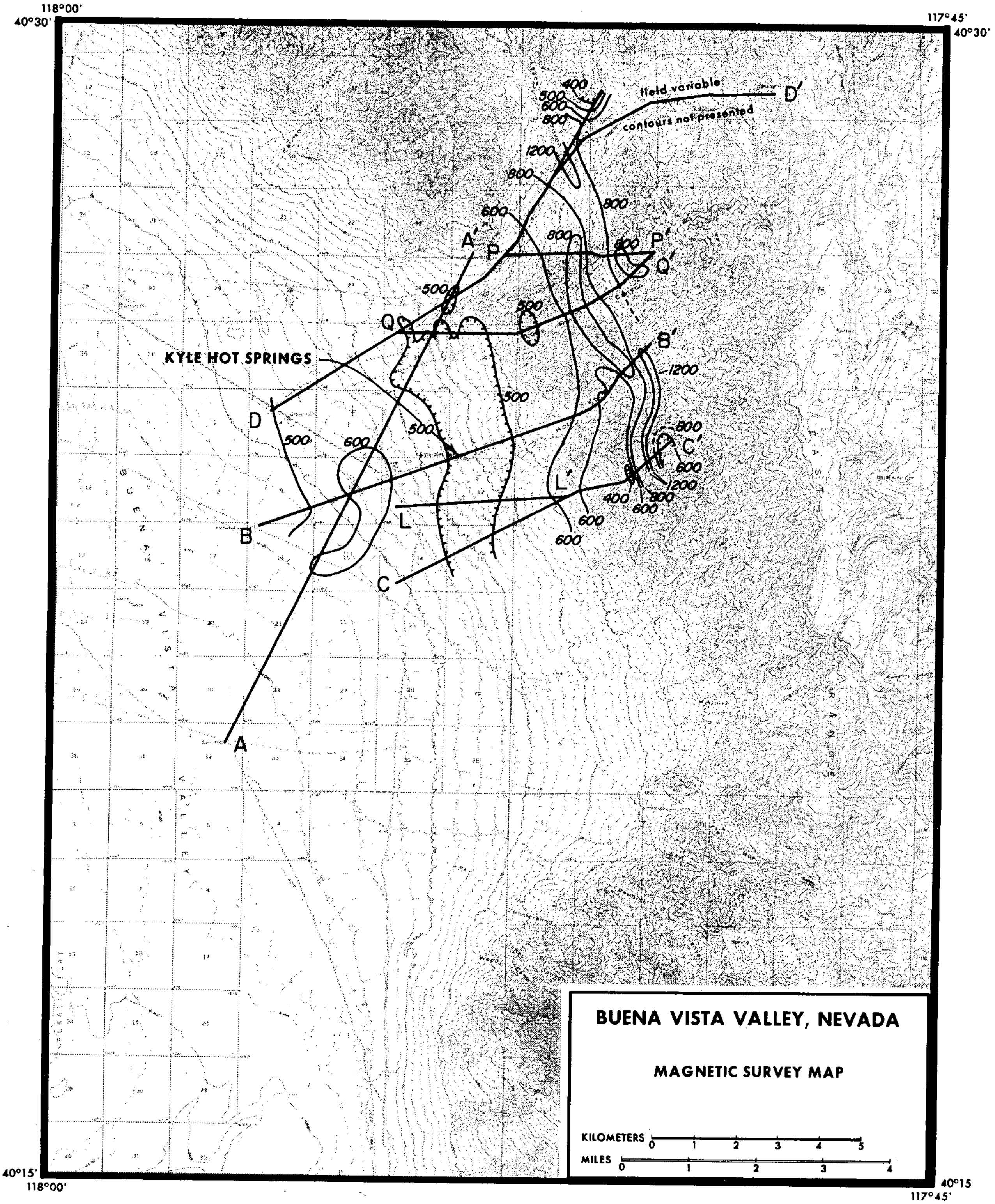

Figure 6 XBL 7612-10925

Magnetic Survey Map; Contoured Values in Gammas.

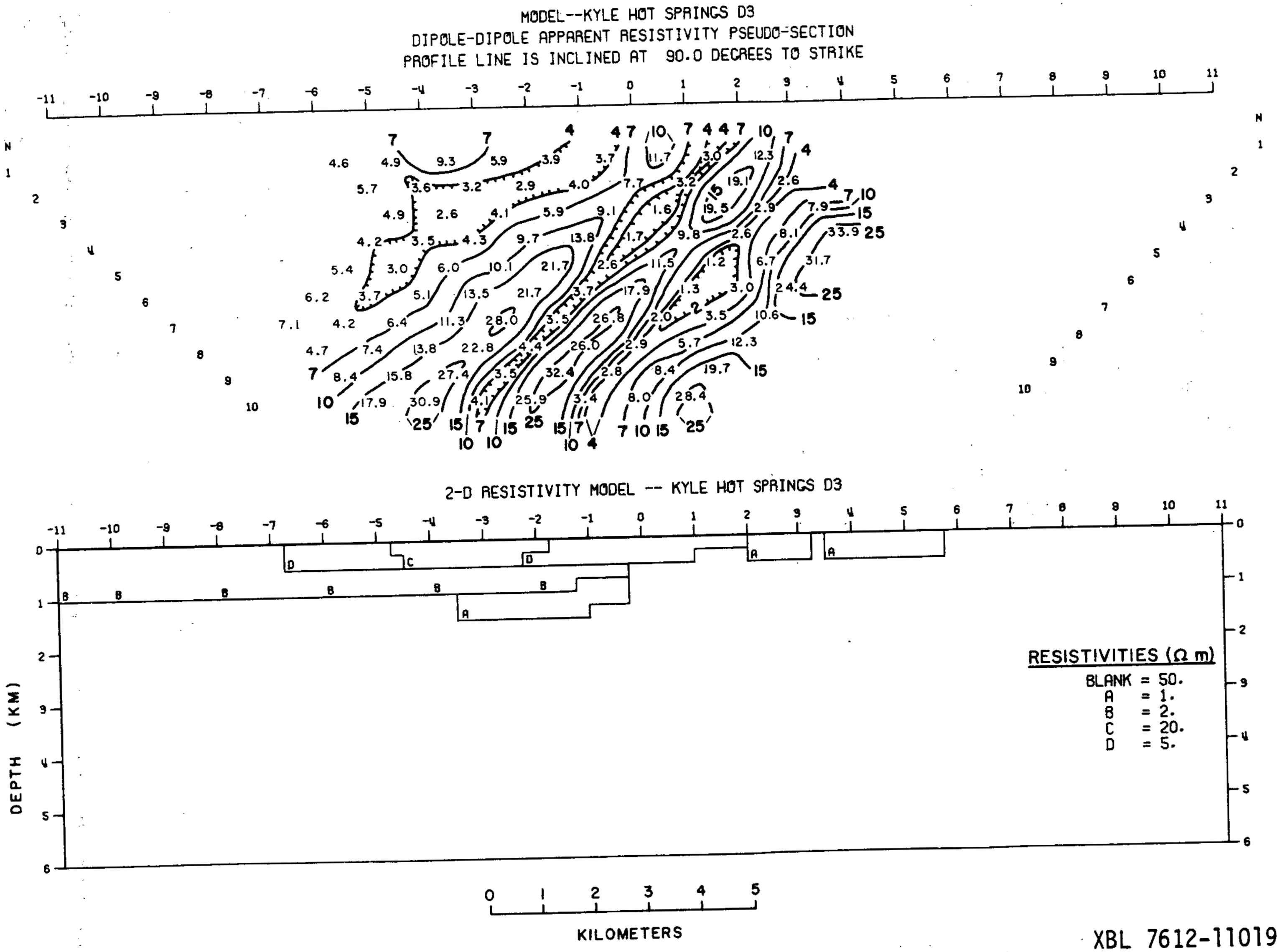

XBL 7612-11019

Figure 7. Dipole-Dipole Apparent Resistivity Pseudo-Section Calculated for the Model Shown, Line D-D'.

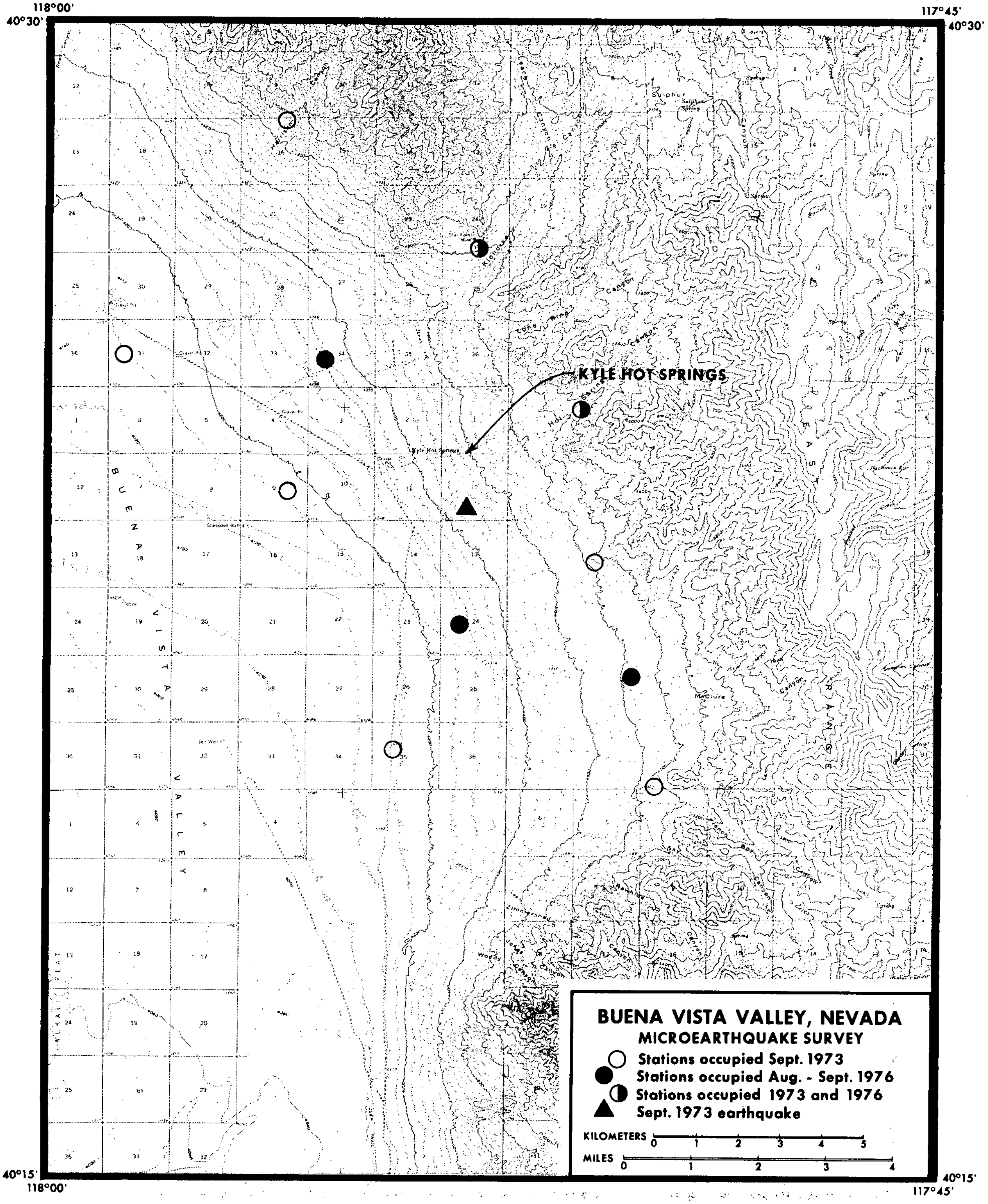

XBL 7612-10922

Figure 8

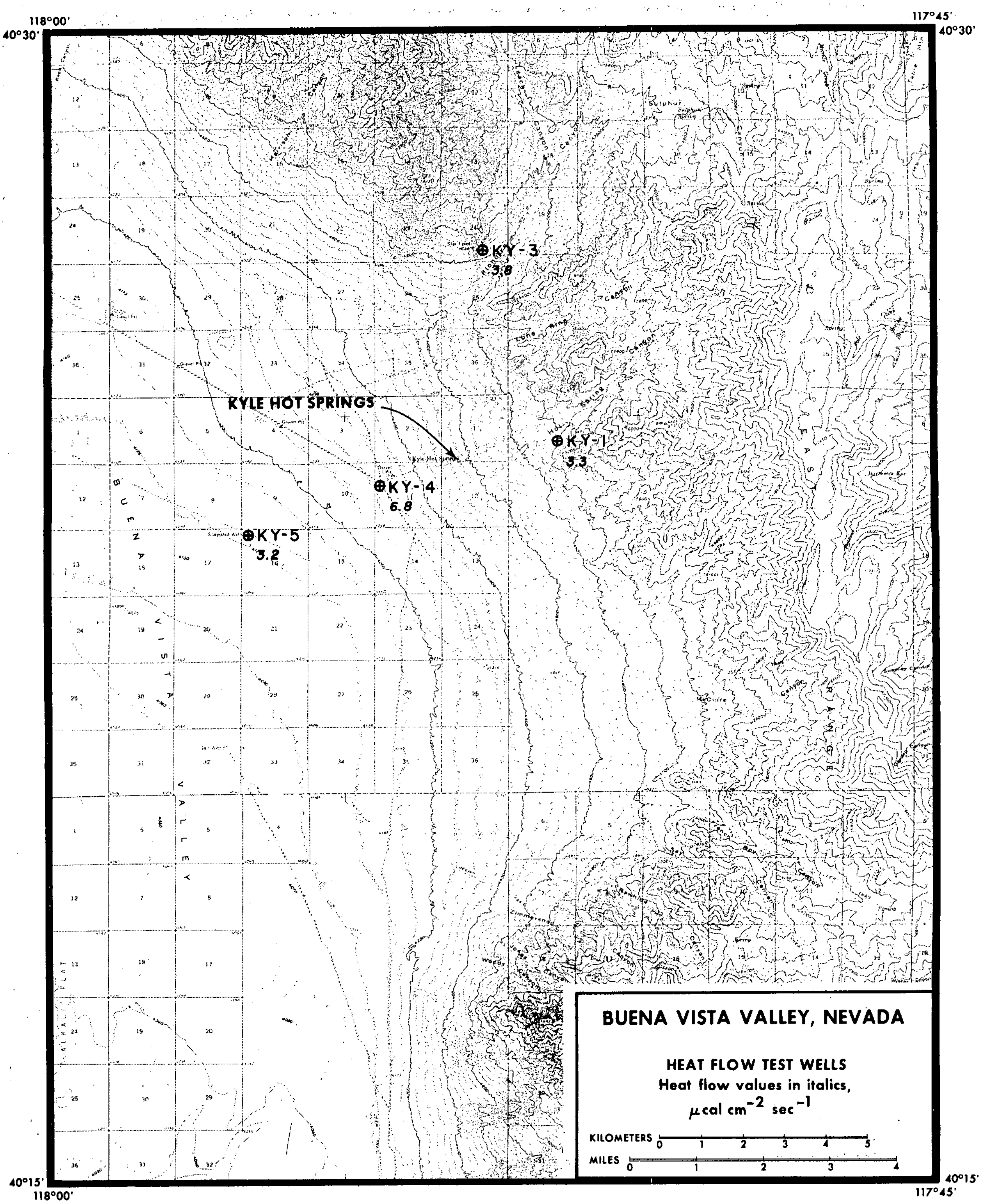

XBL 7612-10924

Figure 9

APPENDIX

GEOPHYSICAL PROFILES

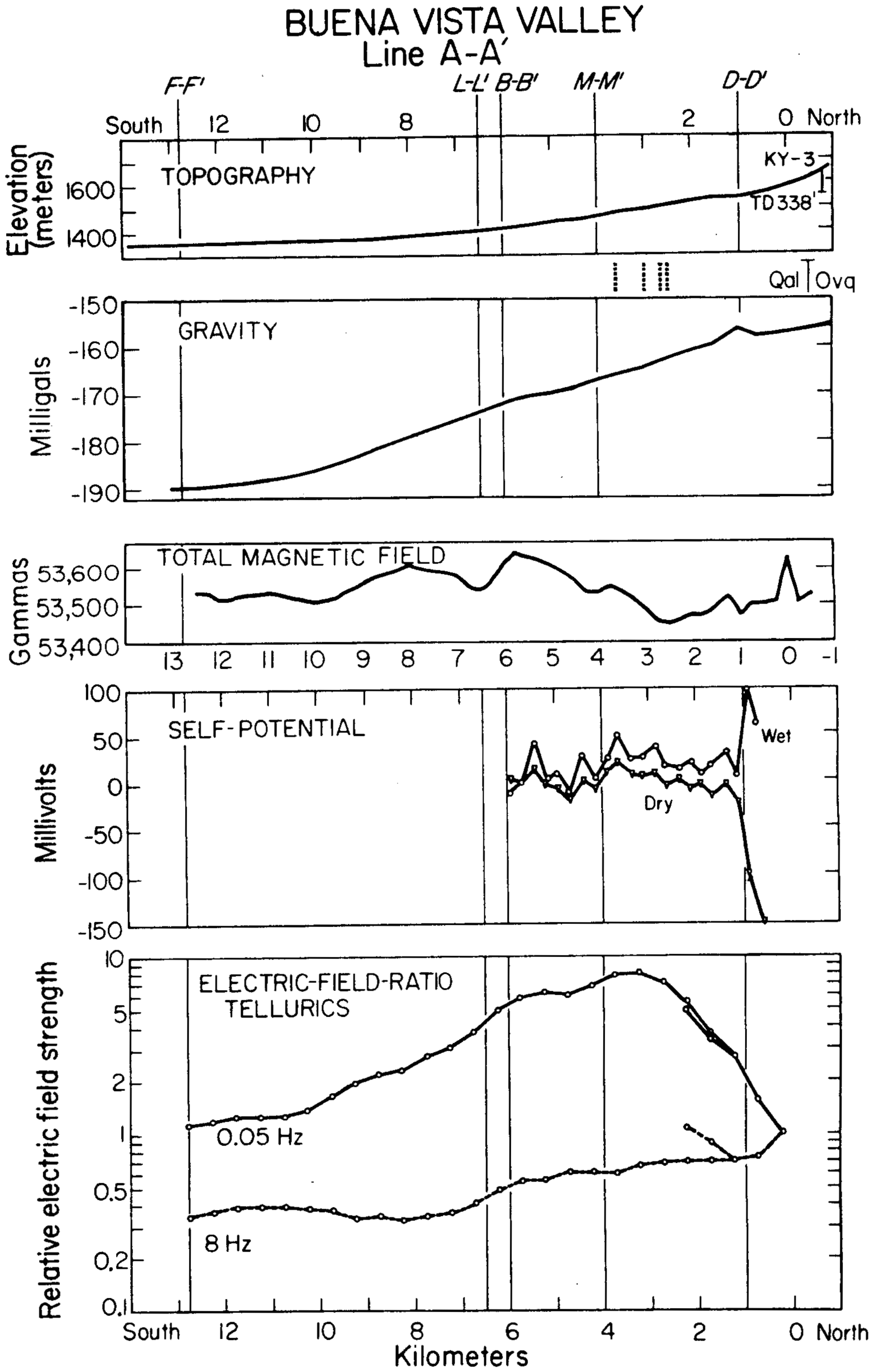

XBL 7612-4501

Figure A1. Geophysical Data Profile Composite, Line A-A'.

Note: Intersecting profile lines are marked above the topographic profile, and geological features are marked above the gravity profile as follows: observed faults, heavy solid lines; inferred faults, heavy dashed lines; lithologic contacts, thin solid lines.

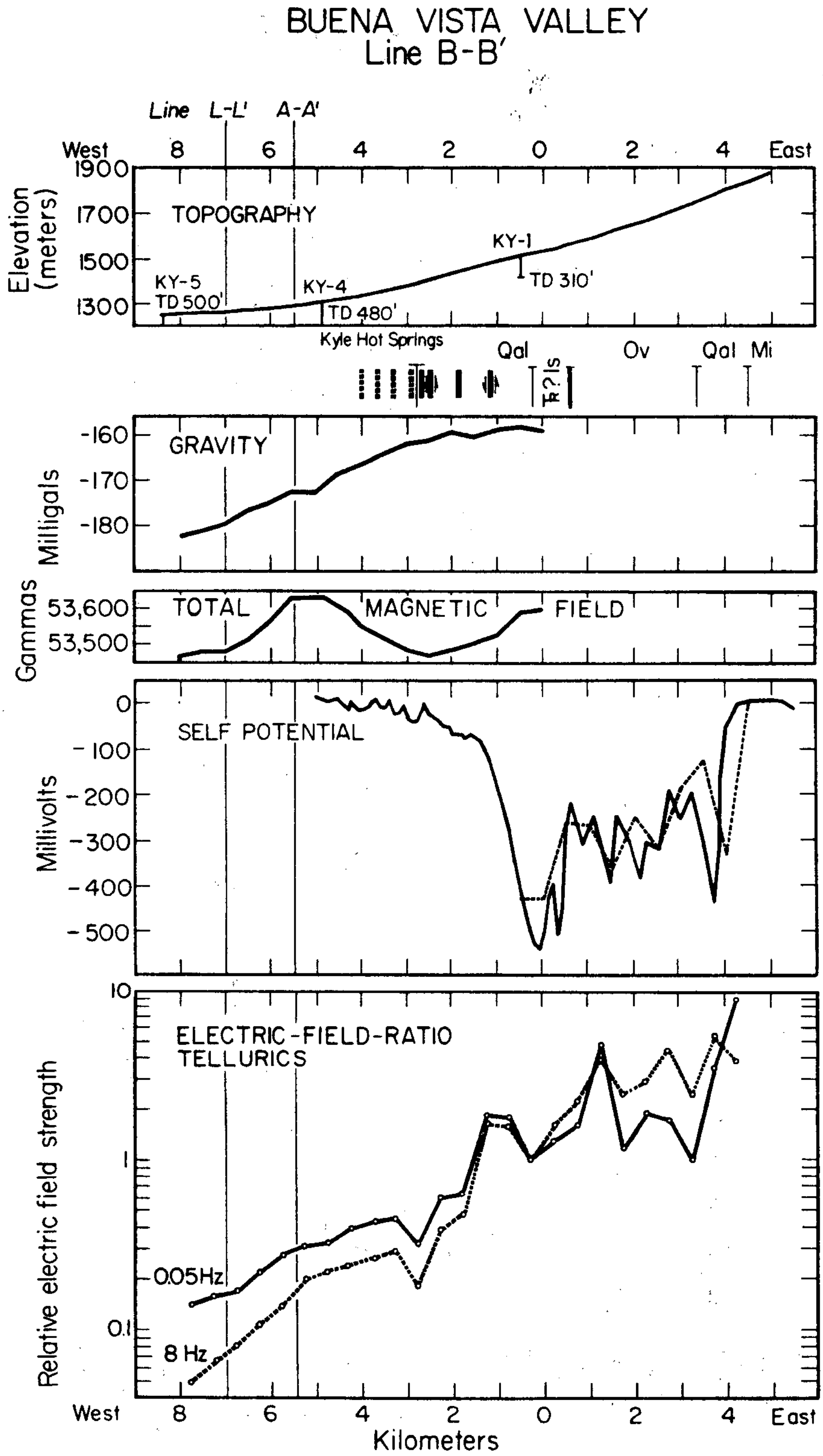

XBL 7512-9824 A

Figure A2. Geophysical Data Profile Composite, Line B-B'. Dotted line on SP profile is from a survey by a second field crew.

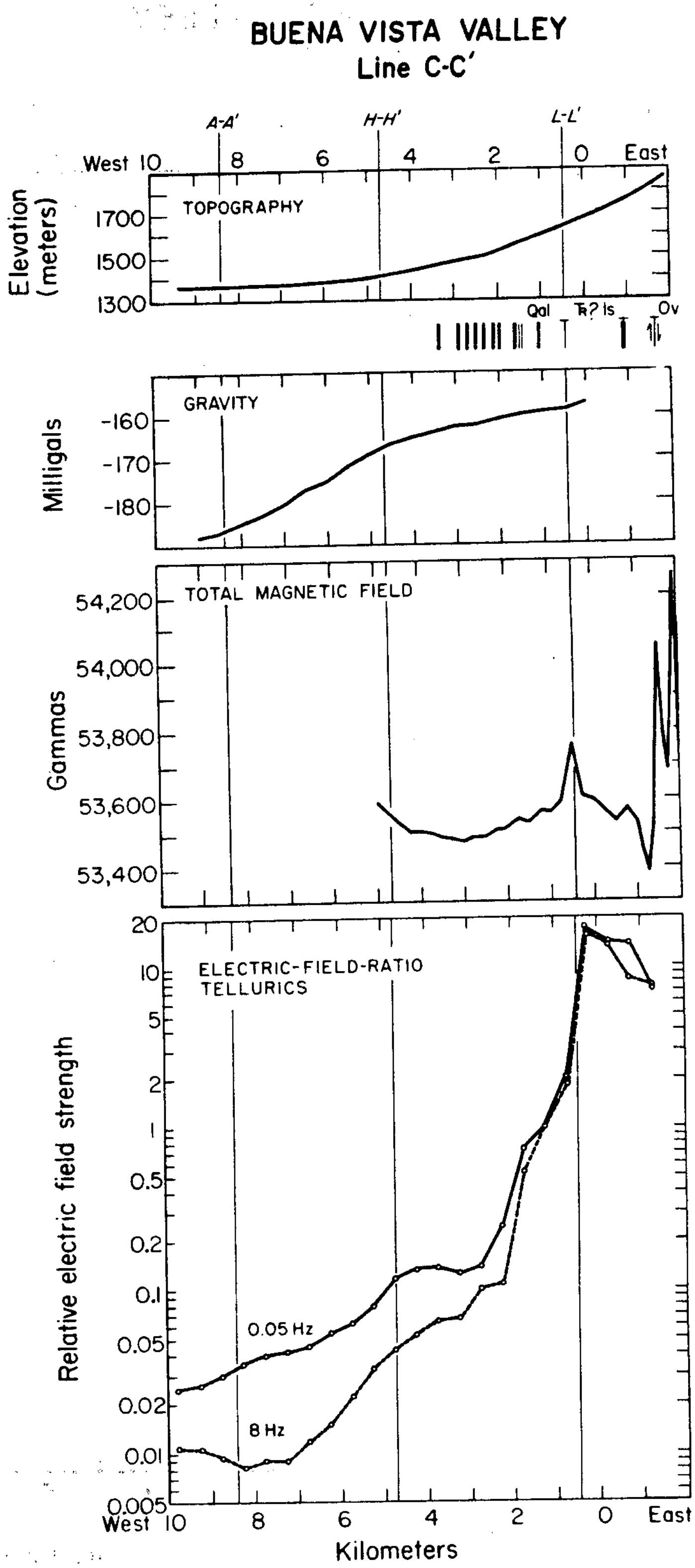

XBL 7612-4502

Figure A3. Geophysical Data Profile Composite, Line C-C'.

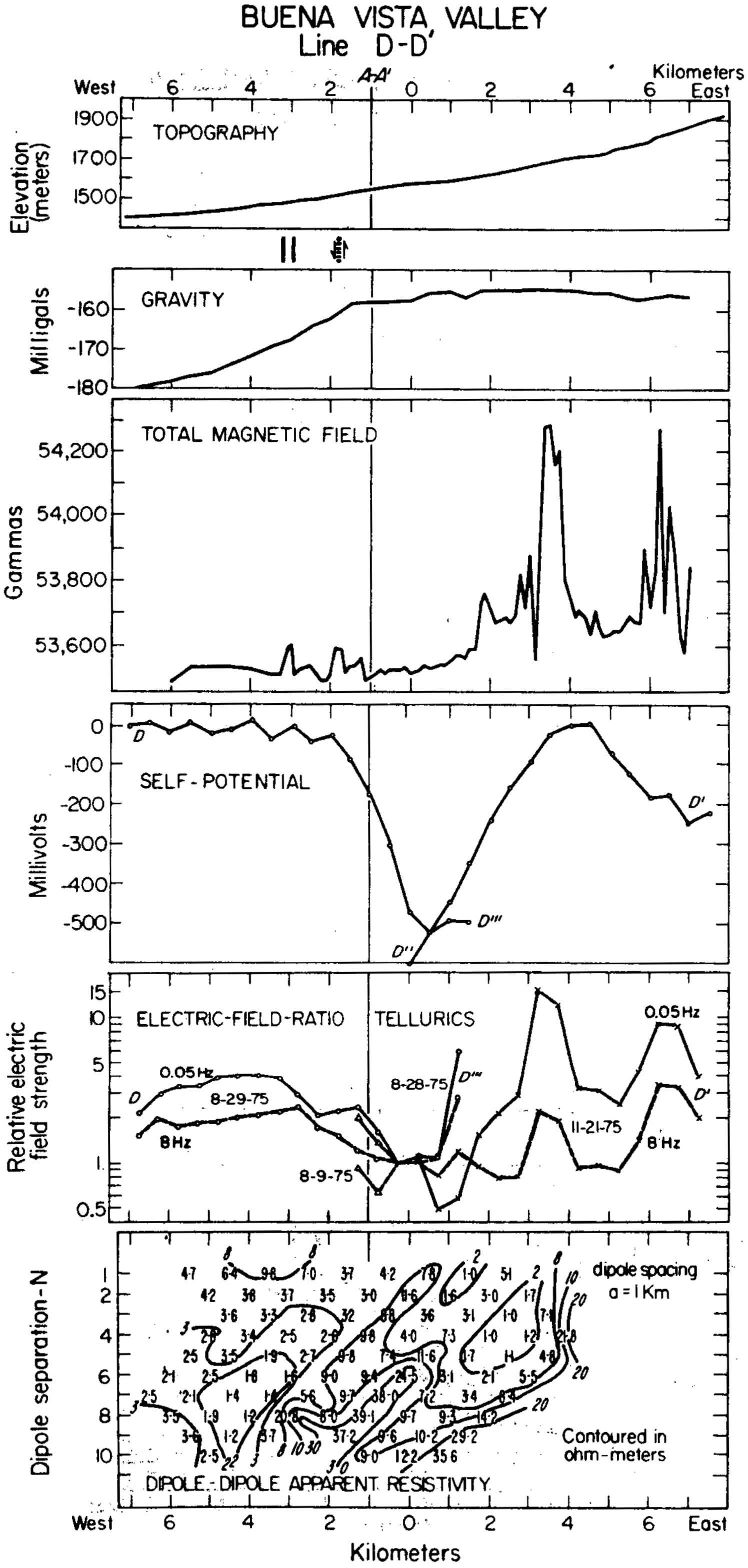

XBL 7512-9835A

Figure A4. Geophysical Data Profile Composite, Line D-D'.

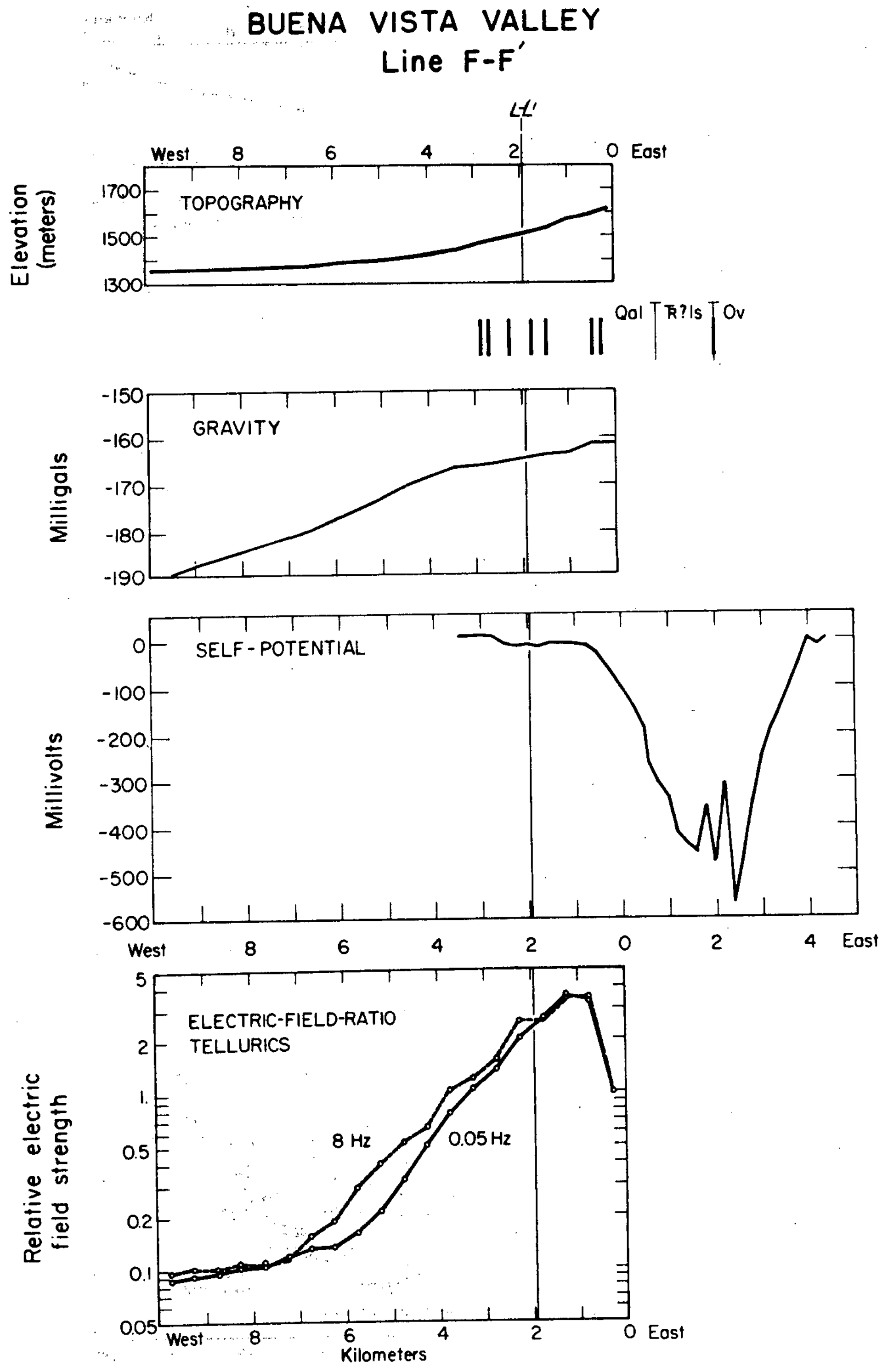

XBL 7612-4507

Figure A5. Geophysical Data Profile Composite, Line F-F'.

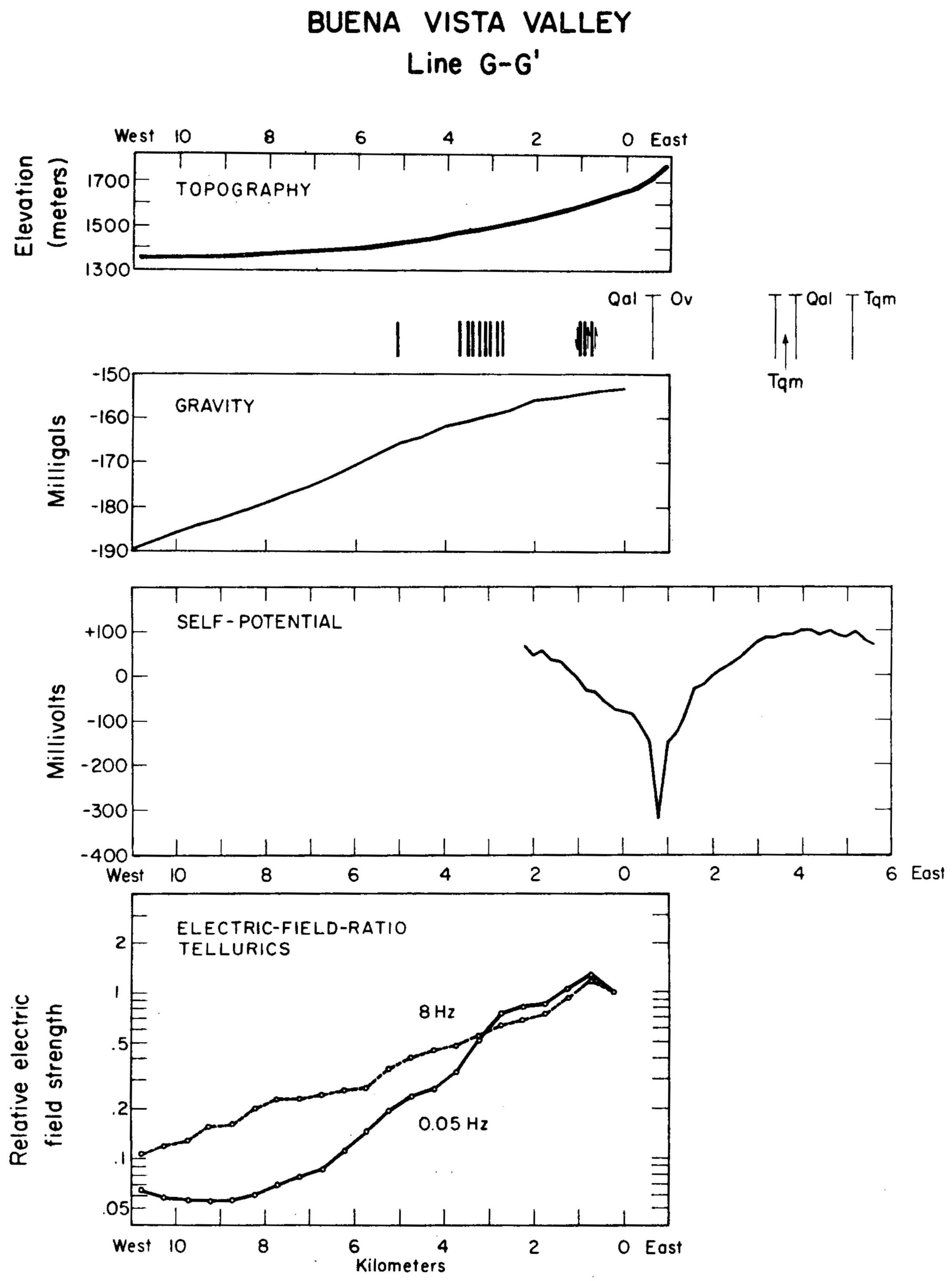

BUENA VISTA VALLEY
Line G-G'

XBL 7612-4505

Figure A6. Geophysical Data Profile Composite, Line G-G'.

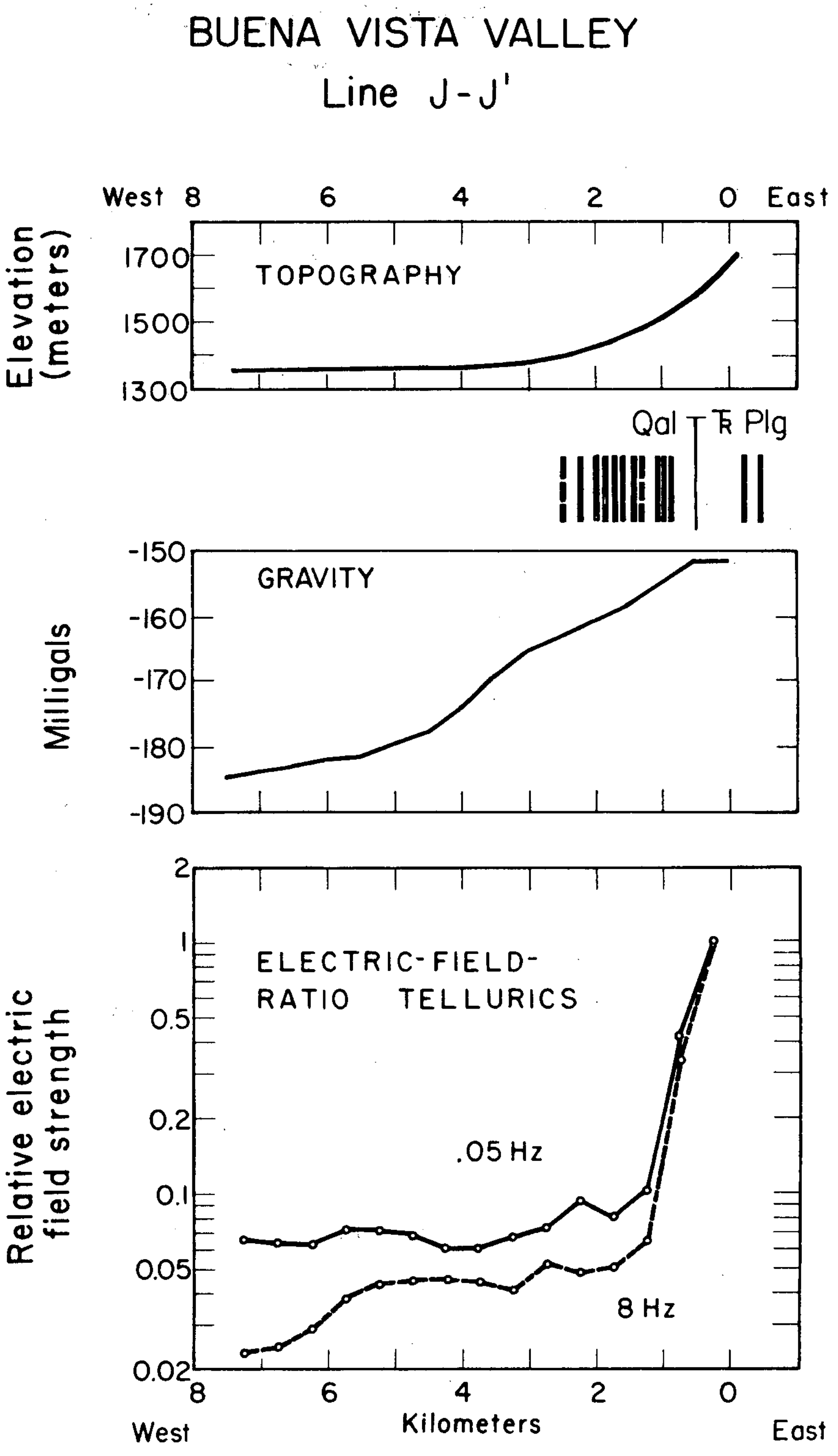

XBL 7612-4506

Figure A7. Geophysical Data Profile Composite, Line J-J'.

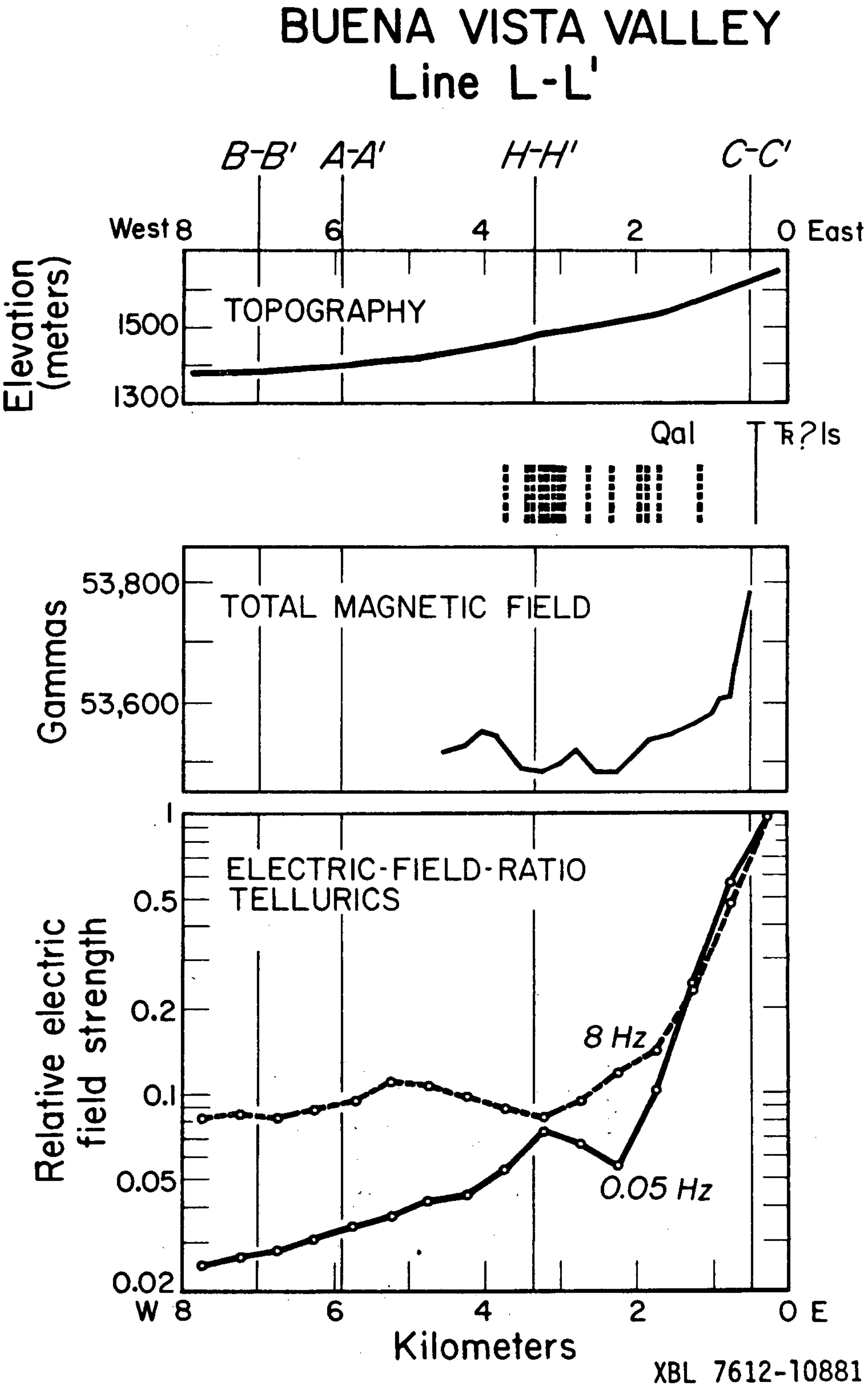

XBL 7612-10881

Figure A8. Geophysical Data Profile Composite, Line L-L'.

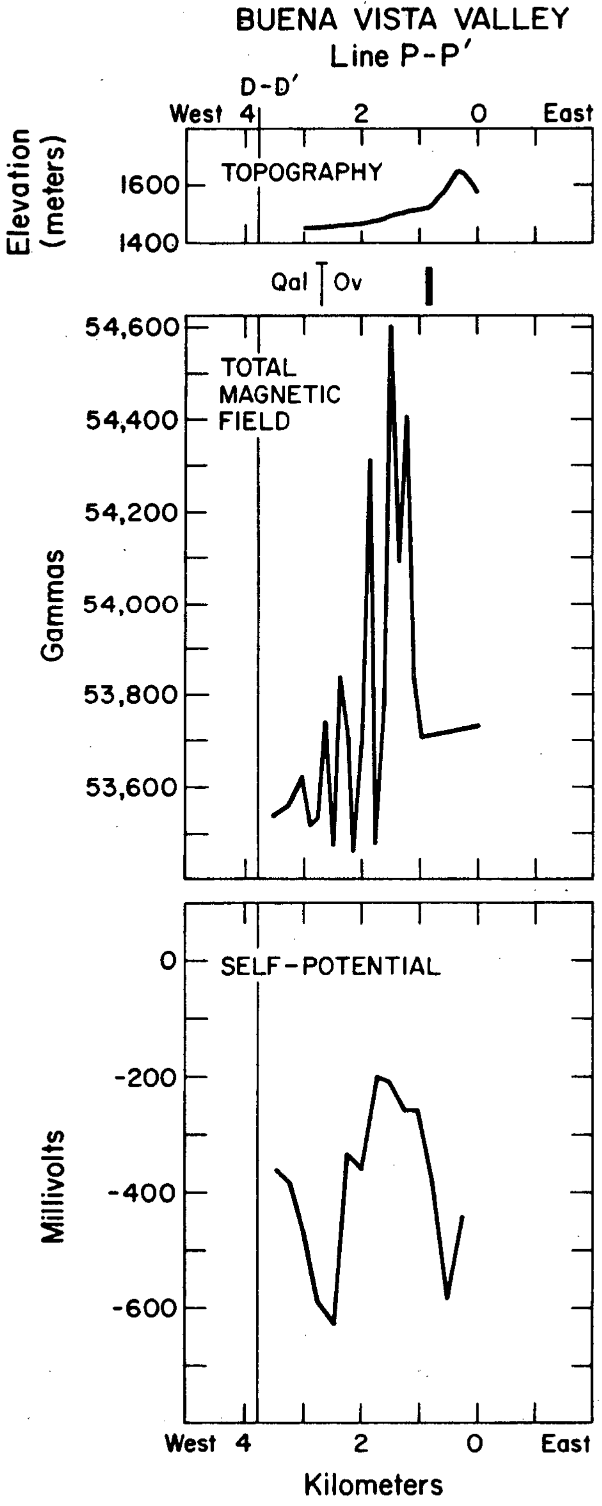

XBL 7612-4503

Figure A9. Geophysical Data Profile Composite, Line P-P'.

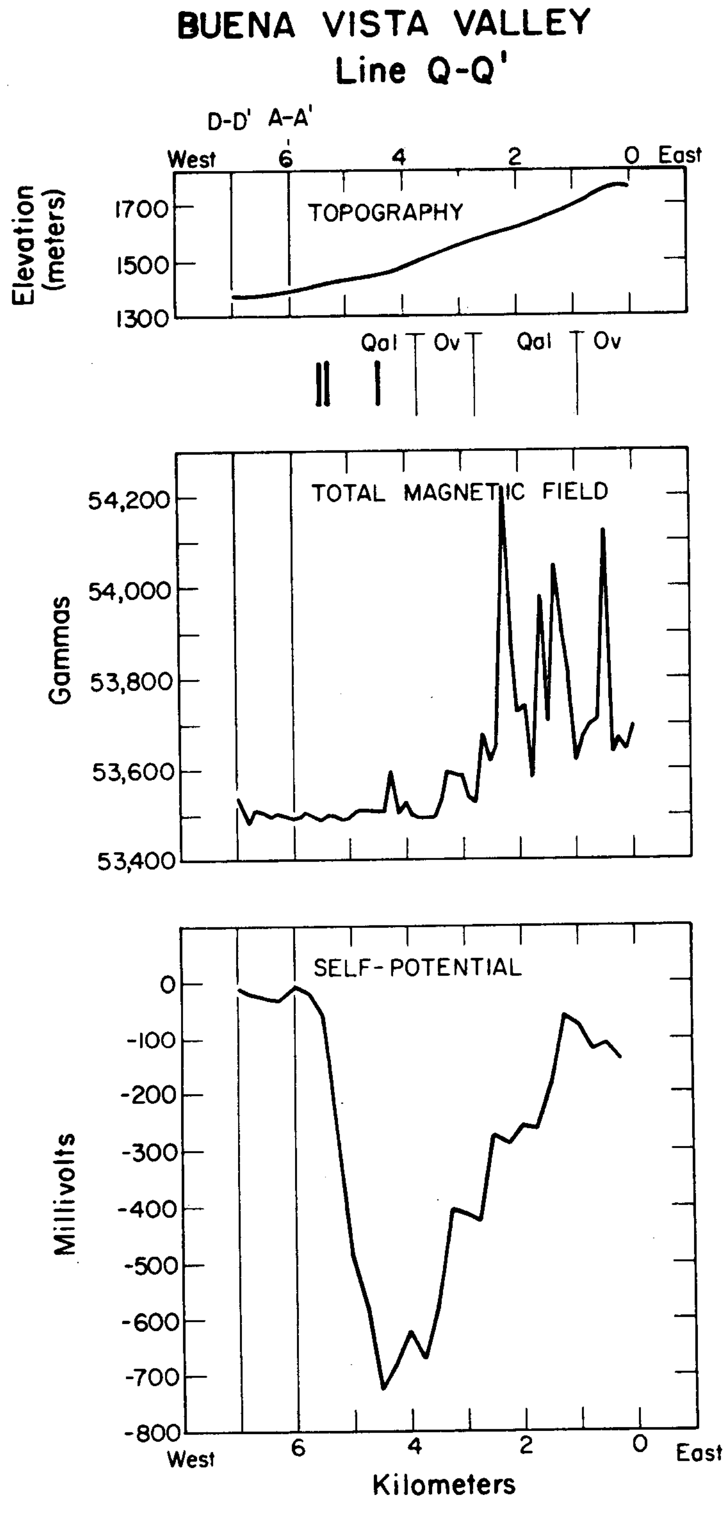

XBL 7612-4517

Figure A10. Geophysical Data Profile Composite, Line Q-Q'.

TECHNICAL INFORMATION DIVISION
LAWRENCE BERKELEY LABORATORY
UNIVERSITY OF CALIFORNIA
BERKELEY, CALIFORNIA 94720